Mason et al. *New Zealand Journal of Forestry Science* (2025) 55:17
https://doi.org/10.33494/nzjfs552025x396x
E-ISSN: 1179-5395
published on-line: 04/11/2025

RESEARCH ARTICLE Open Access

New Zealand Journal of Forestry Science

Modelling above-ground biomass of *Eucalyptus bosistoana* F.Muell. and *Eucalyptus globoidea* Blakely

Euan G. Mason[1,*], Paul Millen[2], Ash Millen[2], Ruth McConnochie[2], Meike Holzenkampfer[1], Monika Sharma[1], Alex Chamberlain[1], James Burns[1], Thomas Copeland[1], Sebastien Lallemant[1], Christophe Robert[1] and Georgia Kennedy[1]

[1] *New Zealand School of Forestry, University of Canterbury, Christchurch, New Zealand*
[2] *New Zealand Dryland Innovation, Marlborough Research Centre, Blenheim, New Zealand*

*Corresponding author: euan.mason@canterbury.ac.nz

(Received for publication 31 May 2024; accepted in revised form 19 August 2025)
Editor: Horacio E. Bown

Abstract

Background: Estimation of forest biomass has become critical as afforestation has been proposed to sequester carbon from the atmosphere in order to mitigate climate change. New Zealand Dryland Forestry Innovation (NZDFI), in collaboration with the University of Canterbury's School of Forestry and the Marlborough Research Centre, has initiated a research and development programme to gather seed, breed, propagate, identify site limitations, model growth, investigate silviculture, and develop wood products from a suite of eucalypts that grow durable heartwood. The aim is to supply naturally durable wood for uses that formerly required either imports of durable wood or copper-chrome-arsenate treated pine.

Methods: As part of a project examining land-use and greenhouse gas budget case studies in Marlborough, New Zealand, we collected and summarised data describing above-ground biomass (AGB) of *Eucalyptus bosistoana* F.Meull., and *Eucalyptus globoidea* Blakely trees across a wide range of combinations of height (h) and diameter at breast height (dbh). One hundred and eleven trees were felled, separated into stems, branches and foliage, and the components were weighed in the field. Subsamples of these tree parts were collected and weighed in the field after separating bark from stem discs. The subsamples were dried in an oven at 105°C, and then weighed. Ratios of dry to wet weights for samples were applied to total green weights from the field in order to calculate AGBs of tree components. Systems of non-linear equations were simultaneously fitted to the data to ensure additivity; that sums of estimates of tree part AGBs versus dhb, h and slenderness (h/dbh) equalled estimates from a model of total tree AGB versus the same independent variables. The study also included the development of a plot-level estimation model of above-ground CO_2-e/ha for *E. globoidea* and its incorporation in an on-line growth and yield simulator. Moreover, a comparison of two pathways to estimating AGB by aerial LiDAR was made: One including estimates of dbh and h from LiDAR and applying the tree-level equations developed in this study, and one going directly from LiDAR metrics to estimates of AGB.

Results: A system of models created for both species with a dummy variable denoting species yielded the least biased residuals, with 22 coefficients estimated in one simultaneous fit. Standard errors varied with plant part and with the size of the prediction, requiring transformations prior to fitting. R^2 values also varied with part, but were typically between 0.96 and 0.98. An exception was foliage and seeds which were influenced by one tree with an unusually high loading of seeds. The standard error for plot level estimates of CO_2-e was 1.9 tonnes CO_2-e /ha and residuals were relatively unbiased. Directly predicting individual tree AGB from LiDAR metrics yielded less biased estimates than predicting dbh and h and then using those estimates to predict AGB.

Conclusions: A system of related, additive equations with a dummy variable denoting species represented the above-ground biomass of *Eucalyptus globoidea* and *Eucalyptus bosistoana* with precision adequate for prediction of biomass for fuel and carbon storage to mitigate climate change. Direct predictions of biomass from LiDAR metrics were less biased than predictions of biomass from tree height and diameter at breast height that were in turn predicted from LiDAR metrics.

Keywords: Keywords: biomass, carbon, additive non-linear equations, durable eucalypts

Introduction

Estimation of forest biomass has become critical as afforestation has been proposed to sequester carbon from the atmosphere in order to mitigate climate change (Obersteiner et al. 2006; Ram Prakash 2010; Aishan et al. 2018). The carbon fraction of forest tree biomass is typically 50% of total biomass (Beets & Garrett 2018; Boucher et al. 2019), and so predictions of total biomass per tree can be easily converted into elemental carbon biomass, and then multiplied by 44/12 to provide estimates of sequestered CO_2, a potent greenhouse gas in our atmosphere. Clearly the denser the wood grown by a tree species, the more potential there may be for carbon storage in forests comprising that species.

New Zealand Dryland Forestry Innovation (NZDFI) imported seed of, and bred, several species of *Eucalyptus* that grow durable heartwood in order to provide naturally posts and poles for New Zealand (Marlborough Research Centre Trust 2023). Two very promising species in New Zealand conditions are *E. globoidea* Blakely and *E. bosistoana* F.Meull. These species tend to grow rapidly (Salekin et al. 2020) and also have dense wood and so they may be ideal for carbon forests and their residues may be a rich source of biofuels (Clifton 1990; Passarella et al. 2023). However, growers require estimates of biomass in order to realise the species' potential for carbon forest or sources of biofuel. Moreover, when these estimates are partitioned by plant part quantities of biomass removed during harvesting, debris available for biofuel, and also leaf area can be determined (Beets et al. 2011). Ideally models of biomass should be created so that foresters can estimate biomass from common measurements such as diameter at breast height (dbh) and tree height (h), and also stand-level estimates obtained from plots, such as mean top height (MTH) (Mason 2019), basal area/ha (G), and stems/ha (N).

Models to predict biomass from tree stem measurements have commonly employed logarithmic transformations and weighted regression to account for non-linearity and heteroscedasticity (Baker et al. 1984; Madgwick 1994). However, Zheng et al. (2015) applied scaled power transformations (Cook & Weisberg 1999), sometimes known as Box-Cox (Box & Cox 1964) transformations, to both dependent and independent variables to stabilise residual variance and linearise relationships between biomass and dbh^2 x h, thereby satisfying assumptions of normality and equal variance required for linear modelling. As models of biomass of plant components are often required, providing consistent estimates of total biomass and sums of component estimates is important.

Ensuring additivity between models of total above ground biomass (AGB) and models of AGB of plant components has generally been achieved in two ways: 1) only models of components are created and then total AGB is defined as the sum of component estimates; or 2) systems of additive equations are estimated simultaneously through joint generalised least squares regression, seemingly unrelated regressions, multi-stage least squares regression or generalised method of moments (Bi et al. 2004; Bi et al. 2010; D. H. Zhao et al. 2015; Daryaei & Sohrabi 2016; Fu et al. 2016; Vonderach et al. 2018; Wang et al. 2018; D. Zhao et al. 2019; Levine & Valpine 2020; Cuevas Cruz et al. 2022). Often total AGB is of prime importance, and so systems of additive equations should be preferred because simply summing estimates of component estimation models may lead to compounded errors. Plot or stand-level estimates of AGB and sequestered CO_2-e may make estimates of sequestration more efficient, and these can be based on tree-level models applied to plots.

Stand- or plot-level estimates of AGB or CO_2-e might be obtained in the same way as stand-level stem volume estimates. If MTH and G are known then stem volume/ha (V) can be directly obtained from equations employing MTH and G as independent variables. Stand-level V equations are usually made by first applying tree-level volume equations (Boczniewicz et al. 2022) to trees in plots, calculating plot-level estimates of V, and then creating models of V versus G and MTH with plots as sampling units. Models of CO_2-e/ha versus G and MTH might be constructed using similar techniques; estimating CO_2-e as 0.5 x AGB x 44/12 (Beets & Garrett 2018) and then fitting models of CO_2-e/ha versus MTH and G.

In order to make assessments of sequestered CO_2-e more efficient, aerial LiDAR estimates of AGB have been explored in a parallel study (Ye et al. 2025), and as New Zealand foresters currently estimate AGB (and CO_2-e) as a function of individual tree dbh and h, it is relevant to ask whether the best use of LiDAR for estimation of sequestered CO_2-e is to use LiDAR estimates of dbh and h and then use current models to estimate AGB (an indirect method), or instead to directly estimate AGB from LiDAR metrics (a direct method).

As part of a project examining land-use and greenhouse gas budget case studies in Marlborough, New Zealand, we initiated a study with the following objectives:

1. Destructively sample *E. globoidea* and *E. bosistoana* trees across as wide a range of dbh and h as possible in Marlborough and North Canterbury and determine the oven-dry biomass in their above-ground components.

2. Create additive models of AGB for whole trees and their components.

3. Create plot-level models of stand-level CO_2-e/ha.

4. Compare indirect LiDAR estimates of tree-level AGB as a function of height and dbh, which are themselves estimated from LiDAR using the models developed in this study with direct LiDAR estimates of tree-level AGB.

Methods

Sites

The NZDFI has a network of over 40 trial sites across New Zealand. A range of landowners, including farmers, vineyard owners, local authorities, and large-scale forest owners and processors are hosting trials on their properties. Trees accessed from nine NZDFI sites were involved in this research, as shown in Table 1 and Figure 1. These sites were selected to provide a broad age-range of trees and because landowners kindly allowed destructive sampling of their trees.

Tree selection

An initial survey of candidate trees was conducted, with vertex measurements of height, d-tape measurements of diameter at breast height at 1.4 m above highest ground level (dbh), and notes of species and location. The aim of selection was to obtain samples from as wide a distribution of tree sizes and height-dbh combinations as possible.

Figure 2 shows the height versus dbh of candidate trees, while Figure 3 shows trees actually sampled. One entire summer between 2022 and 2023 was available, and such sampling is very time consuming, so not all candidate trees could be sampled. For example, just one large tree could take up to three days in the field followed by many hours in the laboratory.

Data describing harvested trees can be found in Table 2. Plantation years ranged from 2003 to 2021. *E. globoidea* planted in 2006 at the MRFP site had the highest average DBH, height, and AGB, and both species at H site had the lowest values due to their young age. At H site, two small *Eucalyptus melliodora* were also sampled, and in addition five trees were added from a previous biomass estimation at Harewood in Canterbury. In addition, data from one *E. globoidea* and seven *E. bosistoana* trees sampled for biomass from Harewood in northern Christchurch were kindly donated to the study (Dr Daniel Bocniewicz, pers. comm.), making a total of 33 and 79 trees for *E. globoidea* and *E. bosistoana* respectively. Trees from Harewood ranged from 5.4-7.0 m in height and 5.15 and 8 cm in dbh. Our trees were sampled for biomass but also for future fitting of compatible stem volume and taper equations. As preliminary taper and volume equations had already been estimated for *E. globoidea* (Boczniewicz et al. 2022) fewer trees of that species were sampled during this study.

Field procedures

The following field procedures were implemented for each sampled tree:

1. Ground line diameter (5 cm above ground) and dbh (cm) were measured.
2. Canopy widths in the two directions NW-SE and NE-SW were measured.
3. The north side of the tree was marked on the bark.
4. The tree was then felled.
5. The tree number was painted on each stump.
6. Diameter over-bark and four bark thicknesses were measured at 0.3 m in taper steps of approximately:
   - 25 mm diameter over-bark if the large-end diameter is 250 mm or less,
   - 50 mm if the large-end diameter is between 500 and 250 mm,
   - 75 mm if the large-end diameter is between 750 mm and 500 mm,
   - so on down to 50 mm, diameter over-bark.
7. If a diameter measurement location happened to be on a heavily branched stem section another location was chosen either above or under the branches and the measurement height was recorded.

TABLE 1: A description of study sites. Elevation information was extracted from the LiDAR data collected in this research. Climate data for the period 1950-1980 were acquired from the New Zealand Environmental Data Stack (NZEnvDS) (McCarthy et al. 2021)

Site Name	Elevation (m)	Temperature (°C)			Total annual Rainfall (mm)
		Minimum during the cold month	Maximum during the warm month	Mean annual	
Fleming and Martin property (FM)	73 - 128	1.6	21.9	11.4	743
Marlborough Regional Forests Pukaka (MRFP)	22 - 115	3.2	22.0	12.4	1183
MacBeth (MB)	104 - 213	0.5	23.1	11.5	902
Marlborough Regional Forests Waikakaho (MRFW)	20 - 67	1.8	23.1	12.4	997
Marlborough District Council Cravens Road (MDCC)	14 - 31	1.7	23.0	12.6	830
Holdaway (H)	287 - 340	-0.5	22.8	11.1	1114
Dillon (D)	218 - 265	-0.1	23.4	11.8	824
Avery (A)	8 - 87	3.4	21.6	12.5	632
Lawson (L)	117 - 177	1.9	22.3	12.2	727

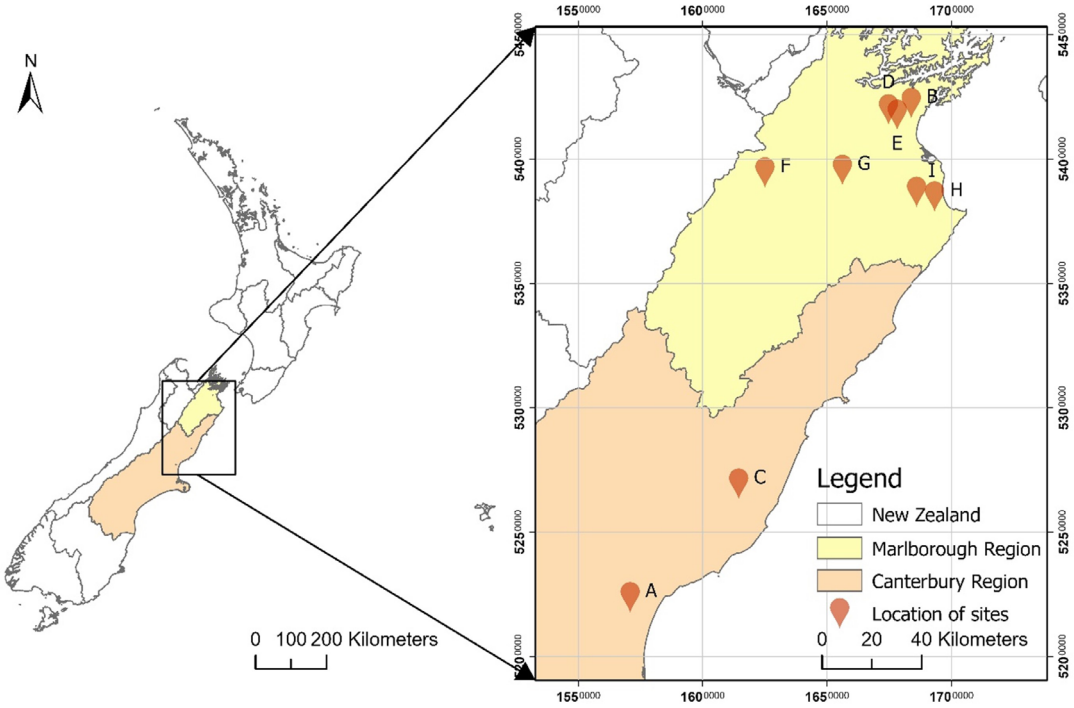

FIGURE 1: Location of sites.

8. The height of diameter measurement was recorded and marked using the colours red (on the bottom), blue (on the top); pattern: 2 cm red – cut mark – 2 cm blue
9. All branches were removed from the stem, and then tree height (m) and height to the base of the green canopy (m) were measured.
10. The stem was weighed and 5 cm thick discs were cut at marked points. Bark thickness was measured on each disk in N, S, E and W directions. Each disk was labelled with tree number, height up the stem and disk number from the base.
11. The wet disks were weighed together or in groups, and then they were debarked and their bark was

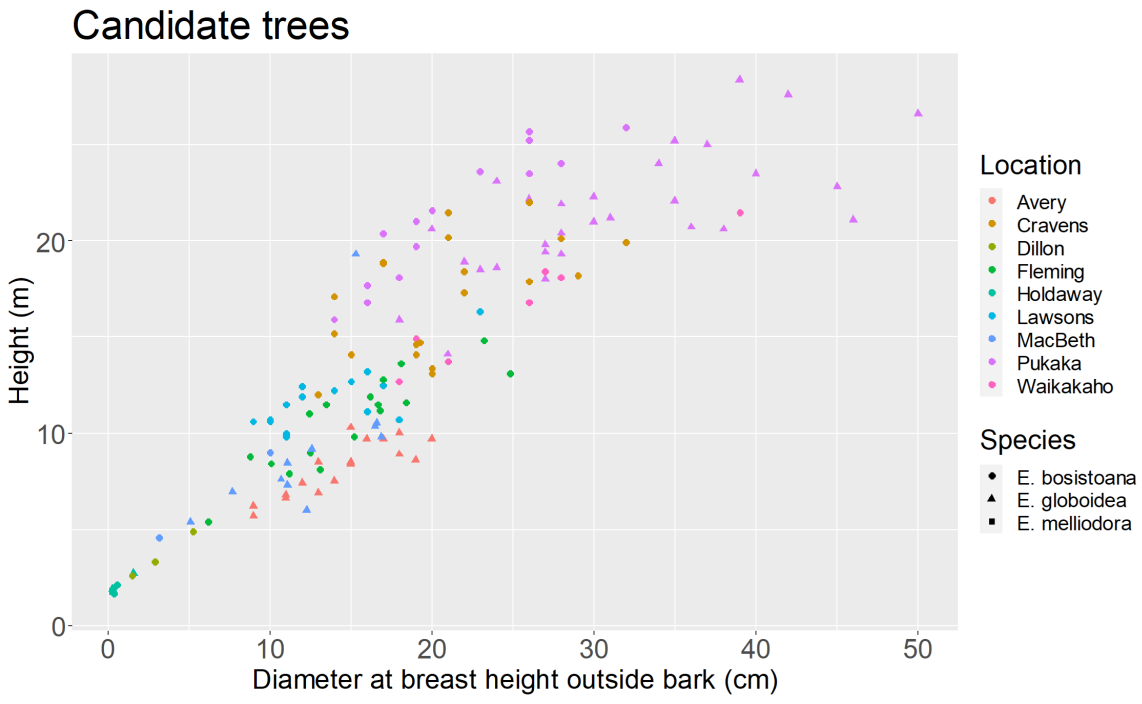

FIGURE 2: Height and dbh of candidate trees identified prior to field sampling

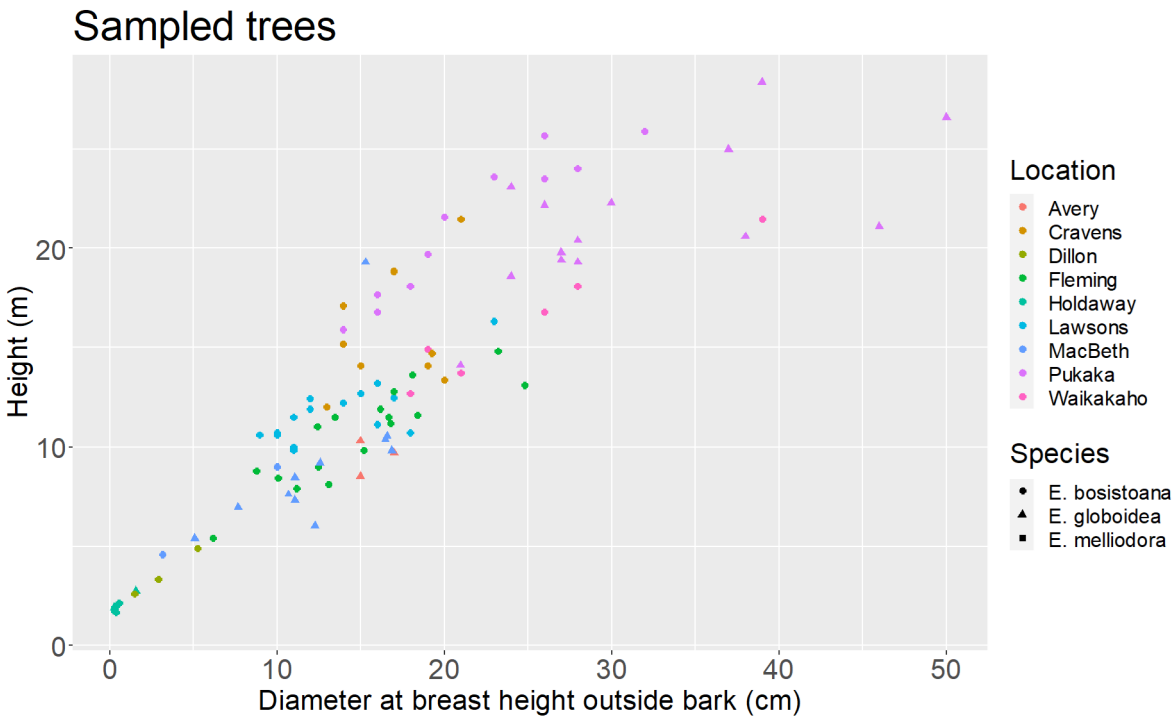

FIGURE 3: Height and dbh of trees sampled during this study

weighed separately. Each disk was stain with methyl red to show where the heartwood was. A graduated ruler was placed on the top of each disk so that heartwood and disk outline could be seen, and the disks were imaged with a digital camera.

12. Bark removed from discs was inserted in a labelled paper bag and the weight of bag plus bark was recorded.
13. Small-leaved foliage, large foliage, and seed capsules were removed separately and weighed, and small samples of small foliage and large foliage for dry mass analysis were in labelled paper bags (about 15 × 15 × 15 cm) which were then weighed.
14. An extra sample (about 10 leaves) of each category of foliage was placed in a labelled, sealed plastic bag for surface area analysis.

TABLE 2: General description of the ground measured trees

Site	Species	Year planted	No. sample trees	Tree height (mean (standard deviation)) (m)	dbh (mean (standard deviation)) (cm)	AGB (mean (standard deviation)) (kg)
FM	*E. bosistoana*	2003/04	17	10.55 (2.38)	14.95 (4.69)	79.68 (72.30)
MRFP	*E. bosistoana*	2003	12	20.84 (3.25)	21.53 (5.50)	210.84 (139.98)
	E. globoidea	2006	13	21.97 (2.64)	32.75 (9.70)	324.17 (215.01)
MB	*E. bosistoana*	2014	3	6.32 (2.35)	6.10 (3.51)	12.40 (14.39)
	E. globoidea		10	8.65 (1.62)	13.08 (3.11)	40.42 (21.32)
MRFW	*E. bosistoana*	2005	6	16.25 (3.47)	25.10 (7.79)	263.58 (242.10)
MDCC	*E. bosistoana*	2009	12	16.41 (3.07)	17.88 (3.17)	118.73 (55.86)
H	*E. bosistoana*	2021	3	1.91 (0.23)	0.47 (0.12)	0.64 (0.17)
	E. globoidea		2	2.32 (0.59)	0.95 (0.92)	1.86 (0.49)
D	*E. bosistoana*	2018	3	3.59 (1.19)	3.23 (1.92)	5.69 (4.29)
A	*E. globoidea*	2011	8	8.87 (1.53)	15.95 (2.82)	47.79 (23.63)
L	*E. bosistoana*	2009	15	11.44(1.48)	13.97 (4.03)	66.21 (39.07)

15. Branches were weighed and then a sample (5 × 15 cm sections) of the branches was placed in a bag for drying. All wet samples and their bags were weighed.
16. A high-quality GPS reading of the tree's location was estimated using a Trimble Geo 7 × global navigation satellite system (GNSS) (post-processed horizontal accuracy ranging from 0.1 m to 1 m). A montage of field procedures is shown in Figure 4.

Laboratory procedures

In a laboratory the following procedures were used to process the samples:

1. A leaf surface area machine was used to measure leaf areas for plastic bag samples, then the leaves were placed in new, small brown bags with the label of tree number, foliage type and "SLA" (because those samples would be later be used to calculate specific leaf area).
2. The volume of each disk was measured by immersion.
3. The brown-bag samples and disks were placed in an oven at 105 °C.
4. A sub-set of the wood samples for each tree was periodically measured to determine when they had stabilised.
5. All dried samples were weighed when the weight had stabilised.

Analysis

Data storage and summarisation

Data were entered into a relational database built for the study, with tables for trees, disks and wood blocks, forms for data entry, and several pre-designed queries so that data could be exported to R statistical software (R Development Core Team, 2004). Tree-level data were then exported to R, and the ratio between subsample dry and green weights was applied to field green measurements of biomass pools in order to calculate the above-ground biomass of stem wood, bark, branches, foliage and seeds. Dry weights of these biomass pools were summed to calculate total aboveground biomass (AGB) of harvested trees.

Modelling individual tree AGB

With such small samples the question arose whether to create separate modelling systems for each species or one combined modelling system with species as a term in the equations. The advantage of separate models would be that relationships between components and stem measures might be quite different between species, but numbers of sampled trees were small especially among large trees because they were so expensive to sample. It was likely that models with small samples might be overly influenced by just a few trees. To compare the two strategies initial, stand-alone models were created for all components and total AGB for each species separately and for the species combined. Model mean standard errors and r^2 values were compared, and also for total tree AGB jackknife (leave one out) validations were conducted and both fitting statistics and residual

FIGURE 4: from left to right, then top to bottom: Tree felled; high quality GPS location; Marking disks to be cut; weighing the whole stem; disks cut; disks collected; note taking; and image of disk stained to show heartwood

plots were examined. As shown in the results section, combined-species models were found to be as precise as separate ones, and were more stable when subjected to validation.

Linear models often require transformations to stabilise variance and make relationships linear. This was very important for our study because relationships tended to be curved and residuals heteroscedastic. Consequently, scaled power transformations were used (Equation 1):

$$x^{(\lambda)} = \begin{cases} (x^{\lambda} - 1)/\lambda & \lambda \neq 0 \\ \log(x) & \lambda = 0 \end{cases} \qquad \text{Equation 1}$$

where x is the variable being transformed, and λ is a parameter that varies usually between -2 and 5, providing a range of transformed shapes. Lambda (λ) values should be chosen to make frequency distributions of variables as normal as possible. A plot of tree AGB versus dbh^2*h (D^2H) was inspected, and following inspection both D^2H and AGB were transformed using scaled power transformations.

Linear models were fitted for the whole tree and for each component with transformed AGB as the response variables, and both transformed D^2H, slenderness (h/dbh) and a categorical variable for species as independent variables. Slenderness was included because it might represent the extent to which trees were growing in a relatively large gap and this might influence allocation of biomass to different components. Models were first fitted with all possible main effects and interactions, and then insignificant model terms, using type 3 sums of squares, were removed sequentially. After each removal the significance of each remaining term was re-examined. The principle of marginality was applied; main effect terms were retained irrespective of their statistical significance ($P<0.05$) if they were present in statistically significant interactions.

Once these models had been fitted command nlsystemfit from the systemfit library (version 1.1) in R (R Core Team 2013) was used to create additive models, using ordinary least squares. Branch AGB was set to the total AGB function minus the sum of all the other functions to assure additivity. Scaled transformed response variables, total AGB and AGB of components stemwood, stem bark, foliage & seeds could only have their best, unique λ values for the transformation included as back-transformations of the right-hand side of the equations, which then placed all the additions in untransformed kg of biomass. The reason for this is that to ensure additivity the dependent variables had to be in the same currency, and their best fit λ values were all different. This strategy retained linearity but would still open small fitted values to possible bias because they would have far smaller residuals than large fitted values. To avoid this bias the models were weighted by d × h, dividing each equation side by d × h. The steps were: 1) Create individual, non-additive models using command nls in R for each component model in order to provide estimates of starting parameters, and then 2) use those starting parameters in nlsystemfit using the ordinary least squares fitting option to create additive models. After models were fitted histograms of raw residuals were examined the ensure they were close to normal, and then back-transformed fitted values and residuals were used to create plots of residuals and also plots of fitted versus actual values that were inspected for bias.

Modelling stand-level AGB and CO_2 sequestered

In order to model above-ground biomass and CO_2 per hectare on a plot basis for *E. globoidea*, permanent sample plot data used by Salekin et al. (2020) were used. The individual tree AGB model developed in this study was applied to each tree in every permanent sample plot (PSP) at each time of measurement, and then these were summed to calculate plot-level AGB at each measurement time in each PSP. Tree heights and dbhs in plots were then used to calculate mean top heights at each measurement time (Mason 2019), along with basal area per plot calculated from dbh measurements. Basal areas and above-ground biomass sums were then divided by plot size to put them on a per hectare basis. AGB/ha was converted from kg into tonnes, divided by 2 to represent elemental C (Beets & Garrett 2018), and then multiplied by 44/12 in order to represent above-ground CO_2-e/ha.

Three different equations (2-4) were evaluated as ways to predict above-ground CO_2-e/ha from basal area/ha (G) and mean top height (MTH).

$$C/G = \alpha + \beta * MTH \qquad \text{Equation 2}$$

$$C = \alpha * G^{\beta} * MTH^{\gamma} \qquad \text{Equation 3}$$

$$C = e^{\alpha + \beta * \log(G*MTH) + \gamma * SDI} \qquad \text{Equation 4}$$

In these equations C=above-ground CO_2-e/ha in tonnes, G=basal area/ha in m^2/ha, MTH = mean top height in m, SDI=Reineke's stand density index (Reineke 1933) and Greek letters are fitted coefficients.

The analyses employed both linear and non-linear mixed effects using the lmer or nlme functions in R packages lme4 (version 1.1) and nlme (version 3.1), depending on the nature of the equation, with plot as a random effect to take account of repeated measures. Model quality was judged by inspecting plots of residuals versus predicted values and calculating standard errors.

Estimation of above-ground biomass using LiDAR

This study combined with our report on the use of UAV LiDAR (Ye et al. 2025) to measure above ground biomass had potential to explore how we might measure CO_2-e stored by forest owners who register their forest stands in New Zealand's emissions trading scheme (ETS). The forest measurement approach to estimation of C sequestration is currently set up to receive measurements of tree stem heights and dbhs which are then used to estimate tree biomass and carbon content. Airborne LiDAR may be a way to acquire estimations more efficiently, but this raises the question of whether LiDAR should be used to estimate heights

and dbhs for the ETS, indirectly assessing biomass and C, or alternatively tree biomass and C should be directly assessed from LiDAR metrics.

It has become clear that LiDAR is good at measuring tree heights, but may be relatively poor at measuring dbhs. There are logical reasons for this:

1. A LiDAR metric called zq95, the height below which 95% of all returns come from a tree is strongly related to tree height, and may differ only slightly with different species due to their different shapes at the tops of canopies (Ye et al. 2025).
2. Dbh is not easily visible from airborne LiDAR, and although oblique LiDAR might help (Justin Morgenroth pers. comm.), the odds are that dbhs of many stems will be undetectable with LiDAR.
3. While foresters routinely estimate heights from trees that have only dbh measurements in inventories, quite commonly the dominant trees in a stand have a wide range of dbhs but more or less the same height, and so it is not routinely feasible to predict dbh from LiDAR height measurements.
4. Indices of competition such as heights of and distances to neighbouring trees, site fertility estimates, and knowledge of stocking management may help somewhat in estimating dbh from LiDAR estimates of height, but these techniques have not yet materialised.

Ye et al. (2025), using the same dataset as ours along with LiDAR metrics for individual trees, reported on a Partial Least Squares Regression (PLSR) model to directly estimate AGB from LiDAR metrics. As reported in their paper:

> "*The surveys were executed using a DJI Matrice 300 RTK equipped with a Zenmuse L1 LiDAR sensor on board. ... The survey employed a single grid flight pattern, capturing triple returns at a sampling rate of 160 kHz. The Zenmuse L1 sensor incorporates a camera that captures the red, green, and blue (RGB) bands. The collected data were pre-processed using DJI Terra 3.11.7.1* (https://www.dji.com/nz/dji-terra), *which included optimising LiDAR point cloud accuracy, smoothing the cloud, exporting the data into the standard format, and reconstructing an orthophoto.*"

They found that a PLSR model best estimated dbh, and a good regression model of tree height versus zq95. We used all these models with ours in this study to compare "indirect" and "direct" estimates of AGB from LiDAR. A "direct" method would predict AGB from LiDAR metrics, whereas an indirect method would involve estimation of AGB from dbh and height that were derived from LiDAR. This was relevant because attempts to use LiDAR for the purposes of the ETS had focussed on models of AGB as functions of tree dbh and height that were themselves estimated from LiDAR.

Results

Modelling individual tree above-ground biomass (AGB)

A graph of AGB versus D^2H is shown in Figure 5. Individual stand-alone models of total AGB/tree for each species were less stable during validation, particularly for *E. globoidea* (residual plots not shown), and component models were similarly precise using combined species models (Table 3). Therefore, a combined species AGB modelling strategy was adopted. The standard errors

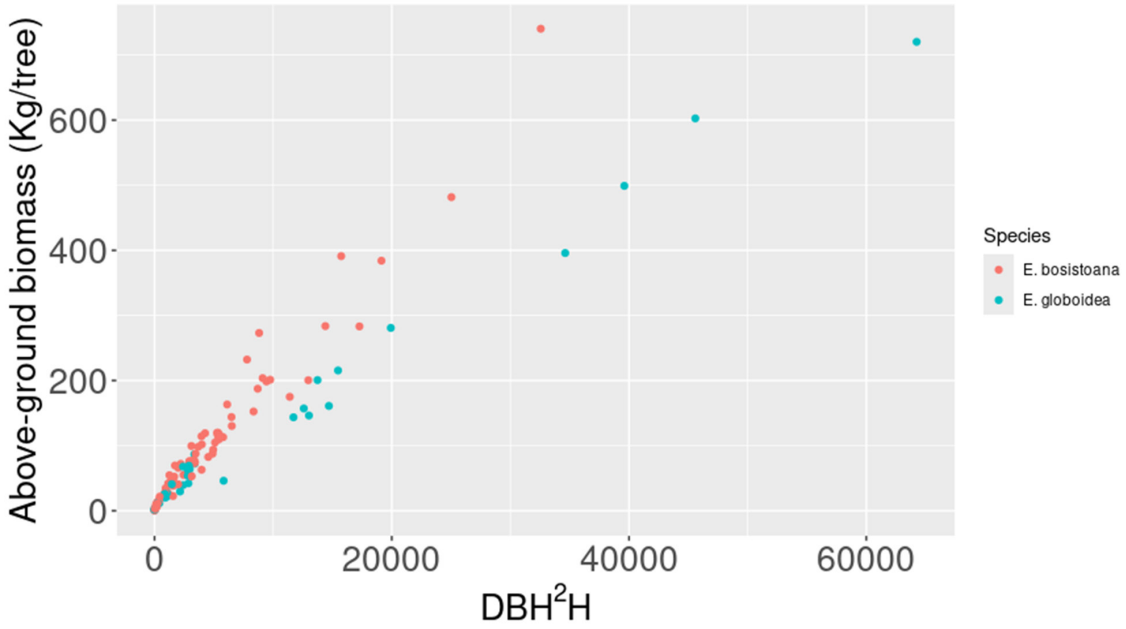

FIGURE 5: AGB versus D^2H by species

TABLE 3: Mean standard errors and r^2 values for unconstrained models of biomass components showing values for joint and separate models for the two species

Component	Species	Standard error (kg)	r^2
Total biomass	Both	21.6	0.977
Total biomass	Both, jackknife validation	23.0	0.973
Stem	Both	13.7	0.978
Bark	Both	3.70	0.961
Foliage and seeds	Both	4.30	0.735
Branches	Both	9.71	0.877
Total biomass	*E. globoidea*	27.0	0.979
Total biomass	*E. globoidea*, jackknife validation	34.2	0.967
Stem	*E. globoidea*	18.3	0.981
Bark	*E. globoidea*	4.55	0.961
Foliage and seeds	*E. globoidea*	3.94	0.859
Branches	*E. globoidea*	10.3	0.829
Total biomass	*E. bosistoana*	21.3	0.971
Total biomass	*E. bosistoana*, jackknife validation	22.8	0.967
Stem	*E. bosistoana*	14.0	0.962
Bark	*E. bosistoana*	3.37	0.959
Foliage and seeds	*E. bosistoana*	3.45	0.894
Branches	*E. bosistoana*	7.20	0.940

shown in Table 3 are mean standard errors after back transformation, and so note that, with heteroscedastic models, larger standard errors would be attached to larger estimates and smaller ones to smaller estimates. Residuals for the combined species model of total AGB along with jackknife (Tukey 1958) residuals are shown in Figure 6. The nlsystemfit procedure involved fitting 22 coefficients simultaneously (Table 4). Plots of residuals versus fitted values and fitted values versus actual values are presented in Figures 7 to 15. One outlier from a large, spreading tree with many seed capsules was detected in the foliage and biomass component model but, as this outlier was real and most other estimates unbiased, we left it in the model.

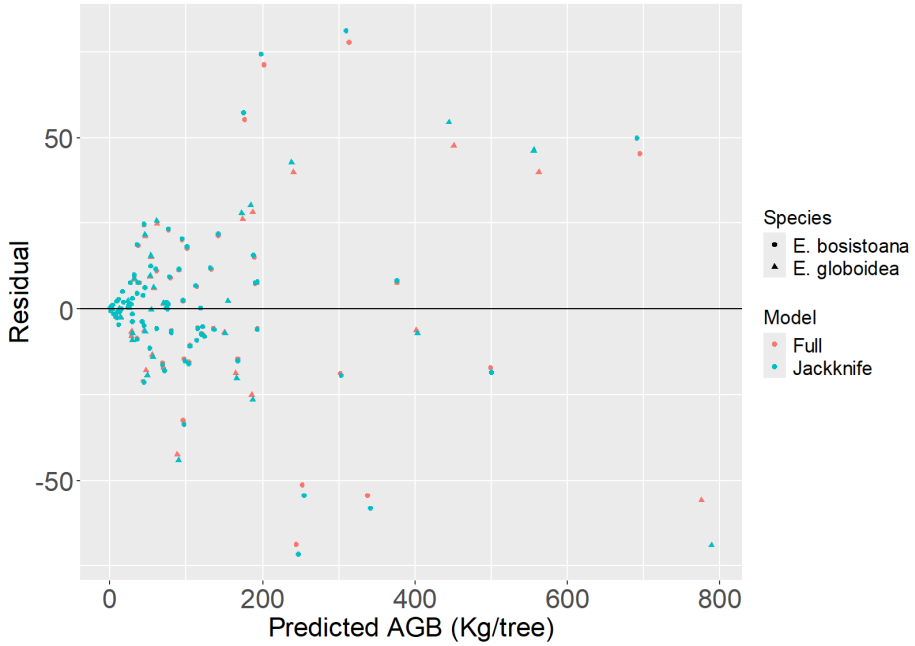

FIGURE 6: Residual versus predicted values of AGB/tree by species, with the full model fit shown blue and the jackknife residuals in red

TABLE 4: Model coefficients and standard errors (in parentheses) and l values

Model	Intercept	D^2H λ=0.24	Species (1 or 0)	h/d λ=-1.27	D2H*Spp	D2H* h/d	h/d* Spp
Total AGB λ=0.17	0.05769973 (1.110e-09)	0.25482753 (5.958e-11)	0.82093885 (8.553e-10)	-0.26895444 (1.530e-09)	-0.05786229 (6.105e-11)		
Stem λ=0.18	-1.39298307 (2.259e-09)	0.26576073 (8.892e-11)	0.62687770 (2.818e-09)		-0.04434272 (1.207e-10)		
Bark λ=0.35	-2.61727152 (9.572e-09)	0.30217405 (9.572e-09)	1.28805265 (1.225e-08)	1.87233580 (1.509e-08)	-0.11871546 (9.962e-10)	-0.02343348 (5.688e-10)	-1.79600684 (1.917e-08)
Foliage & seed λ=0.42	-0.83831203 (8.116e-09)	0.15436852 (6.763e-10)	0.62174469 (1.654e-09)	-0.01437024 (1.311e-08)	-0.01749251 (6.064e-10)	-0.02811382 (6.380e-10)	

Modelling plot-level CO_2-e/ha

Equation 4 provided the least biased and most precise estimate of CO_2-e/ha by a wide margin, and so only the results for that model are reported here. The standard error was 1.92 tonnes CO_2-e/ha, and the residuals were relatively unbiased (Figure 16). Table 5 shows the model's fixed effect coefficients. Note that when applied to plots within the same range but not in the fitting set (i.e.: using just fixed effects) this model would be less precise, with a standard error of approximately 14 tonnes CO_2-e/ha. Using the model outside the range of Salekin et al.'s (2020) growth and yield model would result in an extrapolation and even greater errors. This model was applied in an on-line, plot-level growth and yield simulator for *E. globoidea* which can be found at: http://www.treesandstars.com/euan/egloboidea.htm An output of the model can be seen in Figure 17.

Estimation of above-ground biomass using LiDAR

The indirect pathway for estimating AGB/tree from LiDAR was more biased in this study than direct estimation from LiDAR (Figures 18 and 19).

Discussion

Many previous studies have used additive models to represent biomass of individual trees (Bi et al. 2004; Bi et al. 2010; D. H. Zhao et al. 2015; Daryaei & Sohrabi 2016; Fu et al. 2016; Vonderach et al. 2018; Wang et al. 2018; D. Zhao et al. 2019; Levine & Valpine 2020;

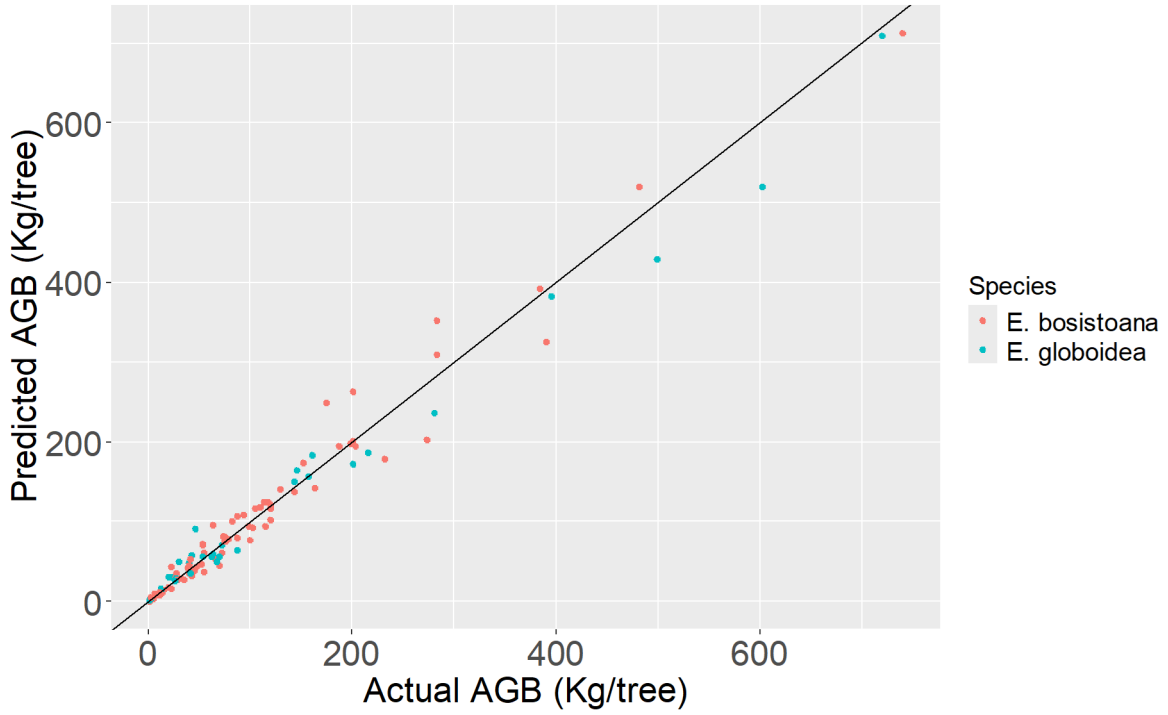

FIGURE 7: Actual versus predicted values of AGB/tree by species for the nlsystemfit model

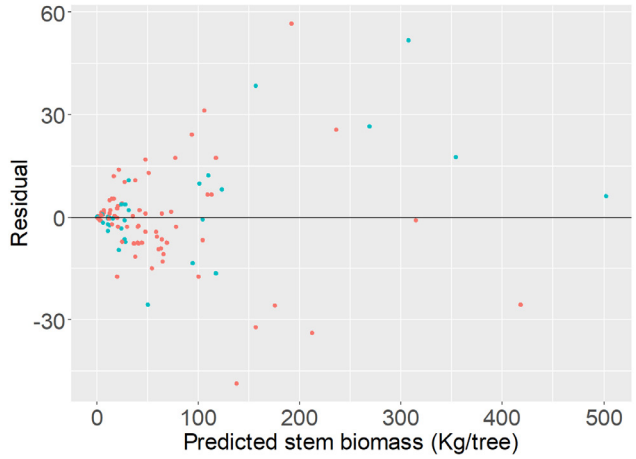

FIGURE 8: Residuals of the predicted stem biomass model fiited with nlsystemfit

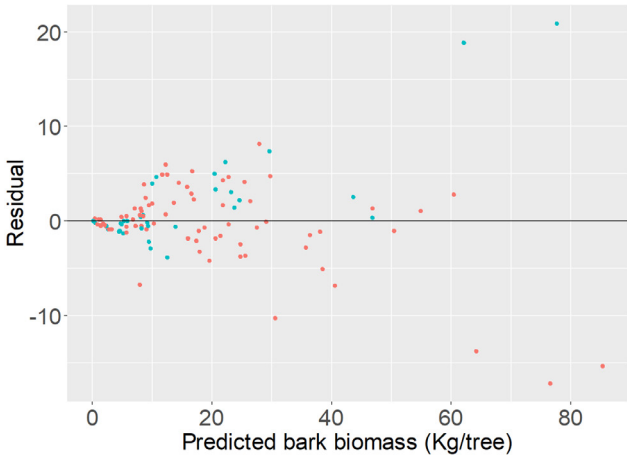

FIGURE 10: Residuals of the bark biomass model fitted with nlsystemfit

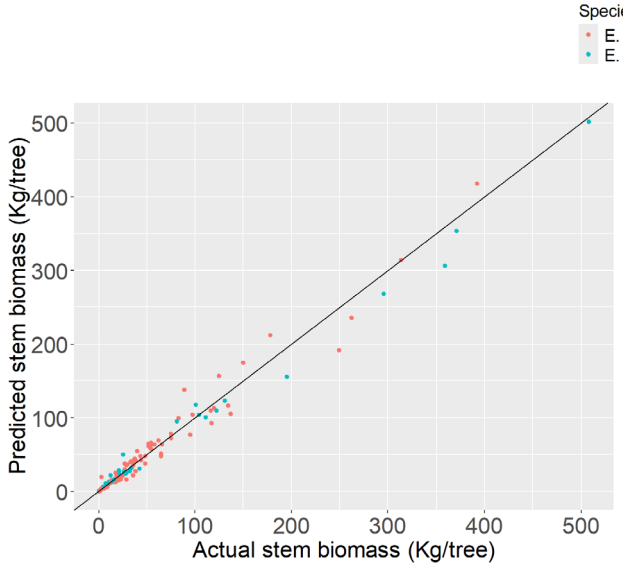

FIGURE 9: Fitted versus actual model for stem biomass

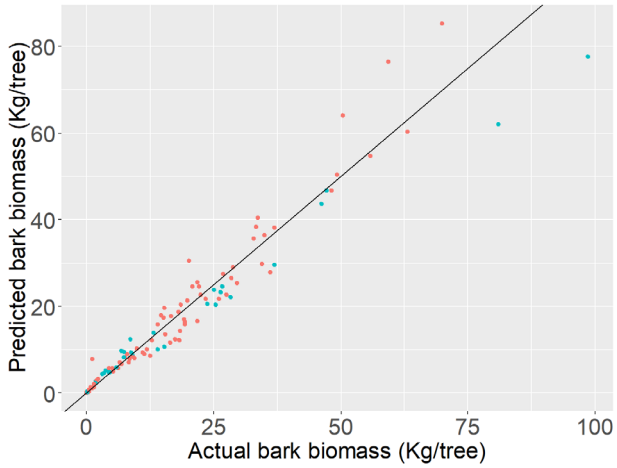

FIGURE 11: Fitted versus actual bark biomass values for the nlsystemfit model

Cuevas Cruz et al. 2022). What is new about this study is combining scaled power transformations of biomass equations (Zheng et al. 2015) with weighted regression to avoid bias, the inclusion of h/dbh to help distinguish spreading trees, and also providing biomass equations for two species whose biomass has not been reported previously and that are becoming important in New Zealand.

A small function has been created in R to report AGBs for any tree within range of the data by its components. The command and output look like this:

```
> predBiomass(25,24,0)
Biomass (kg)        %
Stem                182.77589 60
Bark                54.72537 18
Foliage & Seed      14.92729 5
Branch              53.42213 17
Total               305.85068 100
```

In this case the dbh = 25 cm, the height = 24 m, and the zero denotes *E. bosistoana*. The function is available from the corresponding author.

The models developed during this study have already contributed greatly to the objective of the wider SLMACC project by providing tools to estimate CO_2-e contents of trees and stands of *E. globoidea* and trees of *E. bosistoana* in Marlborough, and also a test dataset for investigating whether or not LiDAR can be used to measure AGB of trees and stands. The data collected will be further analysed to:

- create a set of compatible pool-level ABG equations for the two species
- create models to estimate leaf area index
- improve taper and volume equations that include estimates of heartwood (Boczniewicz et al. 2022)

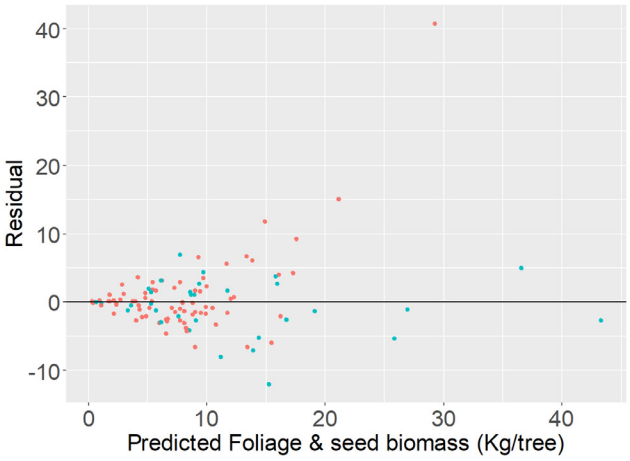

FIGURE 12: Residuals of the foliage and seeds nlsystemfit models

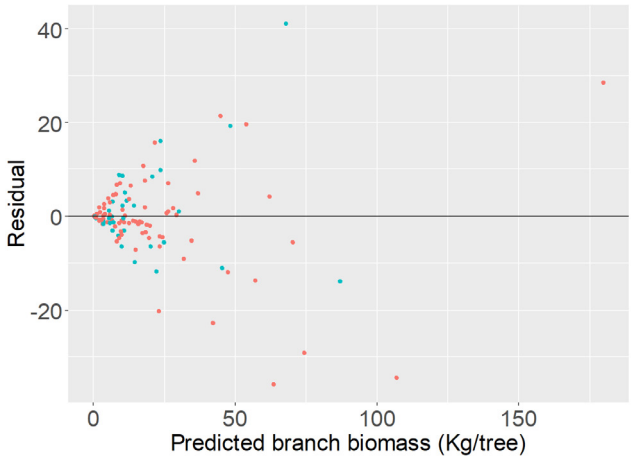

FIGURE 14: Residuals of the branch biomass nlsystemfit model

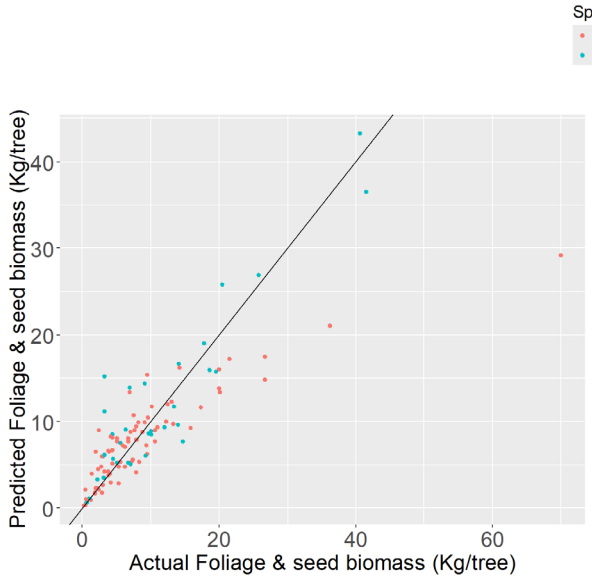

FIGURE 13: Fitted versus actual values of the foliage and seeds model

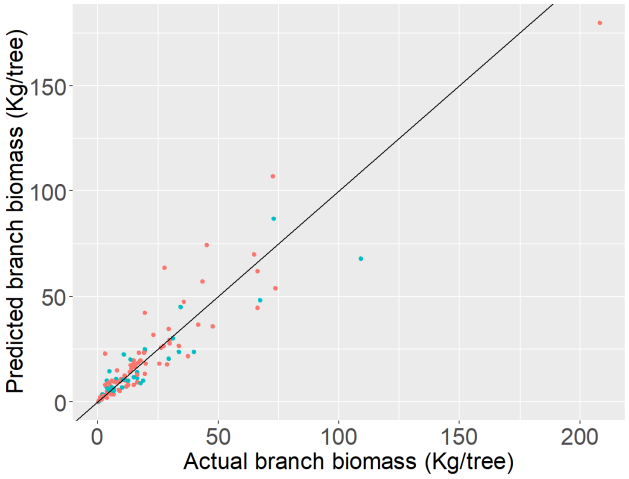

FIGURE 15: Fitted versus actual values of the branch biomass model

- investigate of patterns of wood basic density within stems for the two species
- enable projections for case studies that are the focus of the project of which the study reported here is a part.

A factor pertinent to whether LiDAR should be used to measure AGB directly from LiDAR or indirectly via stem measurements from LiDAR is that for young trees stem biomass is a minority proportion of total biomass, and even for large trees, in the study described here, ~15% of biomass was in foliage and branches, but this percentage was highly variable. Therefore, LiDAR may be useful at helping us to determine a contribution of foliage and branches to biomass which would not be well estimated from only stem measurements. Moreover, from a modelling perspective we should expect that indirectly chaining together several tree models to estimate AGB might result in biased estimates. In this study we created a very good model of biomass versus D^2H. The implication is that directly estimating AGB with LiDAR may be a better strategy than pursuing height and dbh estimates from LiDAR and then using dbh and height to predict AGB. Moreover, as we are interested in stand-level C content for the ETS, individual tree models may be inferior to models that measure C directly from LiDAR metrics for the whole stand.

Conclusions

Individual tree AGB of *E. globoidea* and *E. bosistoana* was found to be well estimated from an equation employing D^2H, h/dbh, and species as independent variables along

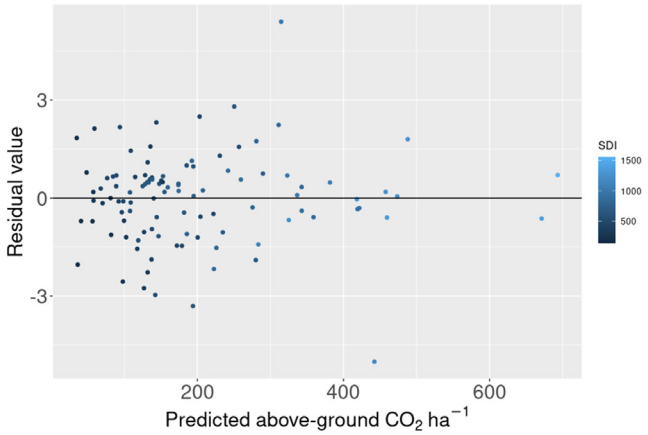

FIGURE 16: Residuals of the plot-level estimation of CO_2-e using equation 4, with plot as a random effect

with their interactions. The R^2 value was 0.98 and the average standard error was 22 Kg, although the standard error when using the model would be smaller for small trees and larger for large trees. Compatible, additive models of tree components were well estimated when all models were fitted simultaneously, providing very high correlations with actual values.

TABLE 5: Fixed effect parameters for Equation 4 after fitting to PSP data

Parameter	Estimate	Std. error	Pr(>|t|)
a	0.2527384	9.761E-02	0.0122
b	0.7389601	1.640E-02	<2.00E-16
g	2.939E-04	1.836E-05	<2.00E-16

Plot-level estimates of above-ground CO_2-e were well fitted to an exponential model that employed MTH, G and SDI as independent variables, and had a standard error when only fixed effects were used of approximately 15 tonnes CO_2-e/ha. This model has been incorporated into an on-line plot-level growth and yield simulator that is freely available to the public.

Direct estimates of AGB from LiDAR were found to be less biased than indirect estimates that used LiDAR estimates of height and dbh and then employed height and dbh to estimate AGB from a model.

Competing interests

The authors have no competing interests.

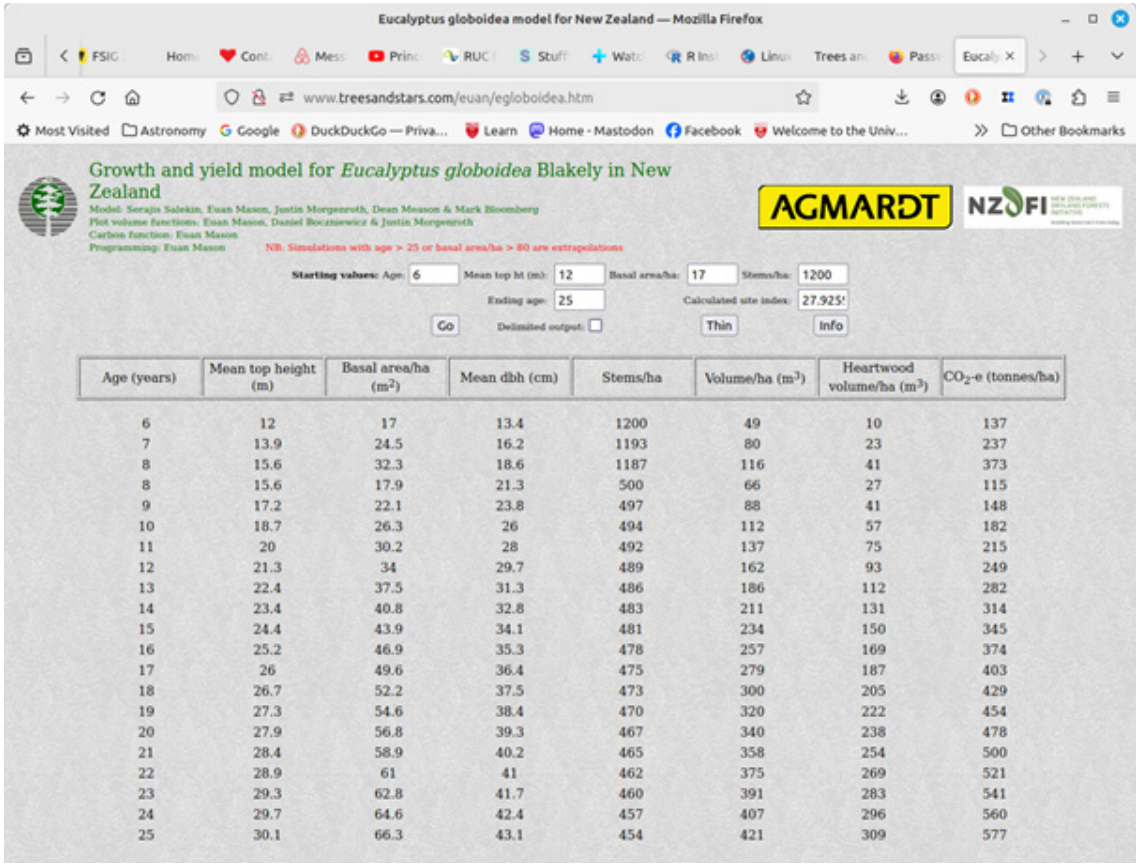

Age (years)	Mean top height (m)	Basal area/ha (m^2)	Mean dbh (cm)	Stems/ha	Volume/ha (m^3)	Heartwood volume/ha (m^3)	CO_2-e (tonnes/ha)
6	12	17	13.4	1200	49	10	137
7	13.9	24.5	16.2	1193	80	23	237
8	15.6	32.3	18.6	1187	116	41	373
8	15.6	17.9	21.3	500	66	27	115
9	17.2	22.1	23.8	497	88	41	148
10	18.7	26.3	26	494	112	57	182
11	20	30.2	28	492	137	75	215
12	21.3	34	29.7	489	162	93	249
13	22.4	37.5	31.3	486	186	112	282
14	23.4	40.8	32.8	483	211	131	314
15	24.4	43.9	34.1	481	234	150	345
16	25.2	46.9	35.3	478	257	169	374
17	26	49.6	36.4	475	279	187	403
18	26.7	52.2	37.5	473	300	205	429
19	27.3	54.6	38.4	470	320	222	454
20	27.9	56.8	39.3	467	340	238	478
21	28.4	58.9	40.2	465	358	254	500
22	28.9	61	41	462	375	269	521
23	29.3	62.8	41.7	460	391	283	541
24	29.7	64.6	42.4	457	407	296	560
25	30.1	66.3	43.1	454	421	309	577

FIGURE 17: The on-line growth and yield simulator for *E. globoidea* that now includes projections of CO_2-e/ha

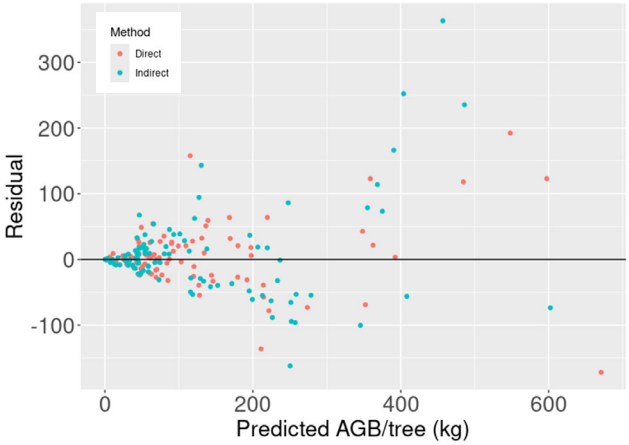

FIGURE 18: Residuals of direct (red) and indirect (blue) estimates of AGB/tree from LiDAR

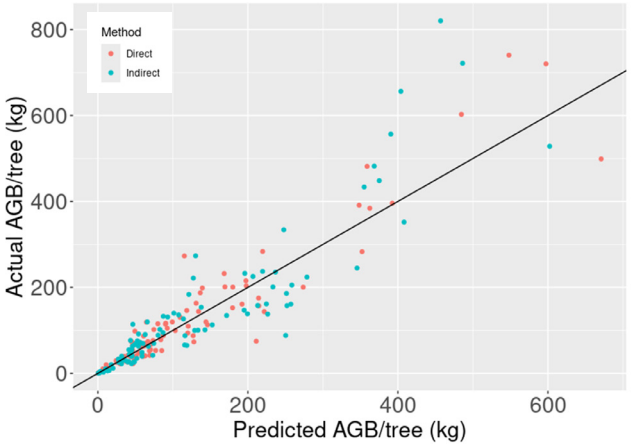

FIGURE 19: Actual AGB/tree versus predicted AGB/tree for direct (red) and indirect (blue) estimation pathways

Author contributions

EM planned the study, helped supervise and conduct the field and lab work, felled some of the trees, created the database, analysed the data, wrote the software and the manuscript. PM, AM, and RMcC located and measured the trees, helped organise funding & accommodation, and helped with tree felling and supervision of field work. MH and MS supervised lab work. AC, JB, TC and SL did much of the field work and organised their activities to a large degree. CR and GK did most of the lab work.

Funding

The authors are grateful for a grant from the New Zealand Ministry for Primary Industries for a grant which enabled this study, grant number SLMACC 406896.

Acknowledgements

The authors thank the land owners who allowed us to harvest trees on their land: Gary Fleming, Marlborough Regional Forests, Robb MacBeth, David & Sue Dillon, Robert Holdaway, Fraser & Shelley Avery, Andrew Lawson, Marlborough District Council and Robert Holdaway. We also thank the New Zealand School of Forestry at the University of Canterbury for paying for staff time to conduct this work.

References

Aishan, T., Betz, F., Halik, U., Cyffka, B., & Rouzi, A. (2018). Biomass carbon sequestration potential by riparian forest in the Tarim River watershed, Northwest China: implication for the mitigation of climate change impact. *Forests, 9*(4). https://doi.org/10.3390/f9040196

Baker, T.G., Attiwill, P.M., & Stewart, H.T.L. (1984). Biomass equations for *Pinus radiata* in Gippsland, Victoria. *New Zealand Journal of Forestry Science, 14*(1), 89-96.

Beets, P.N., Reutebuch, S., Kimberley, M.O., Oliver, G.R., Pearce, S.H., & McGaughey, R.J. (2011). Leaf area index, biomass carbon and growth rate of radiata pine genetic types and relationships with LiDAR. *Forests, 2*(3), 637-659. https://doi.org/10.3390/f2030637

Beets, P.N., & Garrett, L.G. (2018). Carbon fraction of Pinus radiata biomass components within New Zealand. *New Zealand Journal of Forestry Science, 48:* 14. https://doi.org/10.1186/s40490-018-0119-5

Bi, H., Turner, J., & Lambert, M.J. (2004). Additive biomass equations for native eucalypt forest trees of temperate Australia. *Trees: Structure and Function, 18*(4), 467-479. https://doi.org/10.1007/s00468-004-0333-z

Bi, H., Long, Y., Turner, J., Lei, Y., Snowdon, P., Li, Y., Harper, R., Zerihun, A., & Ximenes, F. (2010). Additive prediction of aboveground biomass for *Pinus radiata* (D. Don) plantations. *Forest Ecology and Management, 259*(12), 2301-2314. https://doi.org/10.1016/j.foreco.2010.03.003

Boczniewicz, D., Mason, E.G., & Morgenroth, J.A. (2022). Developing fully compatible taper and volume equations for all stem components of *Eucalyptus globoidea* trees in New Zealand. *New Zealand Journal of Forestry Science, 52: 6*. https://doi.org/10.33494/nzjfs522022x180x

Boucher, J.-F., Tremblay, P., Lefebvre, A., Fradette, O., Bouchard, S., & Lord, D. (2019). The carbon fraction in biomass and organic matter in boreal open woodlands of eastern Canada. *Ecoscience, 26*(4), 309-314. https://doi.org/10.1080/11956860.2019.1586119

Box, G.E.P., & Cox, D.R. (1964). An analysis of transformations. *Journal of the Royal Statistical Society. Series B (Methodological), 26*(2), 211-

252. https://doi.org/10.1111/j.2517-6161.1964.tb00553.x

Clifton, N.C. (1990). *New Zealand timbers: Exotic and indigenous, the complete guide*. Upper Hutt, New Zealand: GP Books.

Cook, R.D., & Weisberg, S. (1999). *Applied regression including computing and graphics*. New York: John Wiley and Sons. https://doi.org/10.1002/9780470316948

Cuevas Cruz, J.C., Aquino Ramirez, M., Ku Chale, R.d.l.C., & Morales Sosa, I.J. (2022). Additive allometric equations to estimate aboveground biomass and carbon concentration of *Piscidia piscipula* (L.) Sarg. *Madera y Bosques, 28*(3). https://doi.org/10.21829/myb.2022.2832356

Daryaei, A., & Sohrabi, H. (2016). Additive biomass equations for small diameter trees of temperate mixed deciduous forests. *Scandinavian Journal of Forest Research, 31*(4), 394-398. https://doi.org/10.1080/02827581.2015.1089932

Fu, L., Lei, Y., Wang, G., Bi, H., Tang, S., & Song, X. (2016). Comparison of seemingly unrelated regressions with error-in-variable models for developing a system of nonlinear additive biomass equations. *Trees: Structure and Function, 30*(3), 839-857.

Levine, J., & Valpine, P.d. (2020). Generalized additive models reveal among-stand variation in live tree biomass equations. *Canadian Journal of Forest Research, 51*(4), 546-564. https://doi.org/10.1139/cjfr-2020-0219

Madgwick, H.A.I. (1994). *Pinus radiata - Biomass, form and growth*. Rotorua, New Zealand: H.A.I. Madgwick.

Marlborough Research Centre Trust. (2023). *About NZDFI*. Retrieved from https://nzdfi.org.nz/about-nzdfi/about-durable-eucalypts/ on 20 November 2023.

Mason, E.G. (2019). Influences of mean top height definition and sampling method on errors of estimates in New Zealand's forest plantations. *New Zealand Journal of Forestry Science, 49:* 1. https://doi.org/10.33494/nzjfs492019x24x

Obersteiner, M., Alexandrov, G., Benitez, P.C., McCallum, I., Kraxner, F., Riahi, K., Rokityanskiy, D., & Yamagata, Y. (2006). Global supply of biomass for energy and carbon sequestration from afforestation/reforestation activities. (Special Issue: Efficient use of biomass for mitigating climate change). *Mitigation and Adaptation Strategies for Global Change, 11*(5/6), 1003-1021. https://doi.org/10.1007/s11027-006-9031-z

Passarella, D., de Carballo, M., Olivera, Y., Bequio, F., Castilho, N., Fabre, C., & Ibañez, M. (2023). Characterization of physical, mechanical and durability properties of *Eucalyptus bosistoana* (F. Muell) cultivated in Uruguay. *Agrociencia Uruguay, 27*. https://doi.org/10.31285/AGRO.27.1293

R Core Team, R. (2013). R: A language and environment for statistical computing.

Ram Prakash, R.P. (2010). Biomass assessment - an unavoidable need for estimating carbon sequestration. (Special issue: Climate change). *Journal of Tropical Forestry, 26*(4), 37-38.

Reineke, L.H. (1933). Perfecting a stand density index for even-aged forests. *Journal of Agricultural Research, 46*, 627-638.

Salekin, S., Mason, E.G., Morgenroth, J., & Meason, D.F. (2020). A preliminary growth and yield model for *Eucalyptus globoidea* Blakely plantations in New Zealand. *New Zealand Journal of Forestry Science, 50*: 2 https://doi.org/10.33494/nzjfs502020x55x

Tukey, J.W. (1958). Bias and confidence in not-quite large samples. *The Annals of Mathematical Statistics., 29*(2), 614. https://doi.org/10.1214/aoms/1177706635

Vonderach, C., Kandler, G., & Dormann, C.F. (2018). Consistent set of additive biomass functions for eight tree species in Germany fit by nonlinear seemingly unrelated regression. *Annals of Forest Science, 75*(2). https://doi.org/10.1007/s13595-018-0728-4

Wang, X., Zhao, D., Liu, G., Yang, C., & Teskey, R.O. (2018). Additive tree biomass equations for *Betula platyphylla* Suk. plantations in Northeast China. *Annals of Forest Science, 75*(2). https://doi.org/10.1007/s13595-018-0738-2

Ye, N., Mason, E.G., Xu, C., & Morgenroth, J. (2025). Individual tree biomass estimation of durable Eucalyptus using UAV LiDAR. *Ecological Informatics, 89*, 11. https://doi.org/10.1016/j.ecoinf.2025.103169

Zhao, D., Westfall, J., Coulston, J.W., Lynch, T.B., Bullock, B.P., & Montes, C.R. (2019). Additive biomass equations for slash pine trees: comparing three modeling approaches. *Canadian Journal of Forest Research, 49*(1), 27-40. https://doi.org/10.1139/cjfr-2018-0246

Zhao, D.H., Kane, M., Markewitz, D., Teskey, R., & Clutter, M. (2015). Additive tree biomass equations for midrotation loblolly pine plantations. *Forest Science, 61*(4), 613-623. https://doi.org/10.5849/forsci.14-193

Zheng, C., Mason, E.G., Jia, L., Wei, S., Sun, C., & Duan, J. (2015). A single tree compatible biomass model of *Quercus variabilis* Blume forests in North China. *Trees: Structure and Function, 29*, 12 pp. https://doi.org/10.1007/s00468-014-1148-1